JOURNAL OF SOLID STATE CHEMISTRY 44, 318-325 (1982)

Mixed Valence Tungsten Oxides with a Tunnel Structure, $P_4W_{4n}O_{12n+8}$: A Nonintegral Member $P_4W_{10}O_{38}$ ($n = 2.5$)

A. BENMOUSSA, Ph. LABBE, D. GROULT, AND B. RAVEAU

Laboratoire de Cristallographie, Physique et Chimie du Solide, L.A. 251, ISMRA, Université de Caen, 14032 Caen Cedex, France

Received February 10, 1982; in revised form May 17, 1982

The mixed-valence oxide $P_4W_{10}O_{38}$, which can be considered as the nonintegral member $n = 2.5$ of the series $P_4W_{4n}O_{12n+8}$, crystallizes in the monoclinic system with unit-cell dimensions $a = 6.5656(25)$, $b = 5.2850(15)$, $c = 20.573(15)$ Å, $\beta = 96.18(4)°$, and space group $P2_1$. The crystal structure was solved by conventional Patterson and Fourier techniques using 2339 counter-measured reflections that obeyed the condition $I > 3\sigma(I)$ and refined to an R factor of 0.074 ($R_w = 0.077$). Basically, the framework of the structure built up from ReO_3-type slabs connected through PO_4 tetrahedra looks like that of $P_4W_8O_{32}$ previously described. Unlike $P_4W_8O_{32}$, two successive ReO_3-type slabs have a different width corresponding to two and three WO_6 octahedra so that the structure can be considered as an intergrowth of the integral members $n = 2$ and $n = 3$ of the series $P_4W_{4n}O_{12n+8}$.

Introduction

The difficulty of adaptation of octahedra and tetrahedra results in few frameworks built up from both sorts of polyhedra that are known at the present time for ternary oxides. In this respect, the ternary system P–W–O offers a perspective of development, since besides the phosphotungstate P_2WO_8 (*1*), two mixed-valence tungsten oxides, $P_4W_8O_{32}$ (*2*) and $P_8W_{12}O_{52}$ (*3*), with a tunnel structure have been recently described. $P_4W_8O_{32}$ differs from the two other oxides in that its framework consists of single PO_4 tetrahedra linked to WO_6 octahedra, while the other oxides are characterized by P_2O_7 groups sharing their corners with WO_6 octahedra. Moreover, the structure of $P_4W_8O_{32}$, which can be described as ReO_3-type slabs, connected through "planes" of PO_4 tetrahedra lets us predict a family of microphases, $P_4W_{4n}O_{12n+8}$. In this series the integer n corresponds to the number of octahedra which determine the width of the ReO_3-type slab, n being equal to 2 for $P_4W_8O_{32}$. The possibility of existence of nonintegral members, which would correspond to the intergrowth of several integral members, has also been considered. The present work deals with the structure of the oxide $P_4W_{10}O_{38}$, which corresponds to the "half integral" member $n = 2.5$.

Experimental Methods

Synthesis and characterization. Preparation of $P_4W_{10}O_{38}$ was made by first heating a finely ground mixture of the appropriate quantities of $H(NH_4)_2PO_4$ and WO_3 in a platinum crucible in air at 673K, in order to decompose the phosphate. The resultant product was then mixed with an adequate amount of metallic tungsten and heated in

0022-4596/82/120318-08$02.00/0

an evacuated, sealed silica tube at 1373K for a week.

A dark blue polycrystalline powder was finally obtained and was mixed with some blue-colored plates. The powder diffractometer data collected with a Philips goniometer and Cu*Kα* radiation were indexed with a monoclinic cell deduced from single-crystal photographs. A least-squares refinement based on 25 reflections was used in conjunction with an index selection program to determine final indices and lattice parameters: $a = 6.5656(25)$, $b = 5.2850(15)$, $c = 20.573(15)$ Å, $\beta = 96.18(4)°$. Density measurements by a pycnometric method led to the observed value 6.04 ± 0.02 in good agreement with the value 6.016 calculated for one molecular unit $P_4W_{10}O_{38}$ per cell.

Determination of the structure. The crystal selected for the structure determination was a rectangular blue plate (110) 6 μm thick.

The intensities were collected on a CAD-4 Enraf–Nonius diffractometer. The data collection's parameters were fixed after a profile analysis of three chosen reflections. The background intensity was recorded on both sides of each reflection and the stability of the crystal was verified with a periodic control. A total of 5163 reflections within a quarter of the reciprocal sphere of radius $\sin \theta/\lambda = 0.995$ Å^{-1} was measured using Mo*Kα* radiation filtered with a graphite monochromator.

The Lorentz and polarization effects were corrected for the 2339 independant reflections which conserved a significant value with $\sigma(I)/I < 0.333$. An absorption correction ($\mu_1 = 430.6$ cm^{-1}) based on the crystal morphology led to transmission factors lying between 0.159 and 0.768.

The two space groups $P2_1/m$ and $P2_1$ agreed with the only observed systematic absences: $0k0$, $k = 2n + 1$. The centrosymmetric group was first considered and the heavy atom methods involving the Patterson function, subsequent Fourier difference maps, and least-squares refinement led to a solution with the conventional $R = 0.075$ and $R_w = 0.078$, all W and P atoms lying in the m mirror. Nevertheless, calculations of the interatomic distances showed abnormal features in this model; in addition, two O atoms exhibited a high isotropic thermal vibration B coefficient. The mean B of the O atoms, indeed, was 1.20 and did not explain the values 3.39 and 2.76 found for O(6) and O(7) atoms in $4f$ sites.

TABLE I

FINAL STATISTICAL TEST

		Theoretical	
	Experimental	Centrosymmetric	Noncentrosymmetric
$\langle E^2 \rangle$	1.0000	1.0000	1.0000
$\langle \lvert E^2 - 1 \rvert \rangle$	0.8239	0.9680	0.7360
$\langle \lvert E \rvert \rangle$	0.8669	0.7980	0.8860

An examination of the Fourier difference maps limited to these oxygen atoms showed clearly doubled maxima for each of them; on the other hand, a refinement made with split positions O(6A), O(6B), O(7A), O(7B) for both atoms gave normal B values and suitable distances. A possible explanation was to consider that these split positions were due to the presence of the m mirror in the space group. Consequently, we assumed that the structure was pseudocentrosymmetric, this point of view being suggested by statistical tests (Table I). All the coordinates were thus refined in $P2_1$ except for the y coordinate of the W(1) atom which has been blocked (Table II).[1]

Final R ($R = 0.074$, $R_w = 0.077$) were of the same order as that of the previous work, but all the interatomic distances were now correct (Table III). For suitable com-

---

[1] The table of F_0 and F_c is available at the laboratory.

TABLE IIa

FRACTIONAL ATOMIC COORDINATES AND THERMAL PARAMETERS WITH ESTIMATED STANDARD DEVIATIONS IN PARENTHESES (SPACE GROUP $P2_1$)

Atom	x	y	z	B_{eq} (Å)
W(1)	0.5392(2)	0.25	0.10908(6)	0.37(1)
W(2)	0.4714(2)	0.2585(9)	0.38890(6)	0.39(1)
W(3)	0.1785(2)	0.2575(9)	0.53569(7)	0.27(1)
W(4)	0.8898(2)	0.2587(9)	0.68304(5)	0.39(1)
W(5)	0.1496(2)	0.2471(9)	0.96227(6)	0.43(1)
P(1)	0.7874(13)	0.2596(34)	0.2641(4)	0.46(11)
P(2)	0.7468(12)	0.2300(22)	0.8402(3)	0.34(9)
O(1)	0.3552(46)	0.2311(78)	0.0349(14)	0.63(31)
O(2)	0.7008(42)	0.2347(94)	0.1948(14)	0.75(33)
O(3)	0.6067(52)	0.2413(199)	0.3080(16)	1.17(37)
O(4)	0.3175(51)	0.2302(69)	0.4605(16)	0.79(37)
O(5A)	0.6850(64)	0.5154(74)	0.0854(21)	0.81(42)
O(5B)	0.7092(51)	0.0214(58)	0.0754(17)	0.39(32)
O(6A)	0.3580(57)	0.4722(70)	0.1547(18)	0.71(37)
O(6B)	0.3839(75)	0.9578(95)	0.1404(24)	1.23(52)
O(7A)	0.9355(81)	0.0437(99)	0.2805(25)	1.25(58)
O(7B)	0.9066(95)	0.5097(107)	0.2728(29)	1.52(67)
O(8A)	0.6154(70)	0.5303(91)	0.4208(21)	0.98(46)
O(8B)	0.6665(71)	0.0403(89)	0.4278(21)	0.99(46)
O(9A)	0.3123(80)	−0.0184(81)	0.3523(23)	0.94(46)
O(9B)	0.2600(63)	0.4809(67)	0.3420(18)	0.58(36)
O(10)	0.9812(52)	0.4664(66)	0.4948(16)	0.67(36)
O(11)	0.9565(71)	0.2383(329)	0.8802(21)	1.83(64)
O(12)	0.7794(44)	0.2702(64)	0.7695(13)	0.57(37)
O(13)	0.0332(52)	0.2546(107)	0.6131(16)	0.98(39)
O(14)	−0.0067(94)	0.4641(86)	0.0041(27)	1.27(58)

parisons with the hypothetical centrosymmetric model the notation of the split atoms are maintained. So, O(5) gave rise to both positions O(5A) and O(5B). For the nonsplit atoms, essentially only y coordinates were modified and an examination of Table II gives an idea of the deviation from the centrosymmetric results. It must, however, be pointed out that the esd on y coordinates close to $y = 0.25$ are systematically higher than that on x coordinates, while the cell parameters are similar. These results might be related to the very low deviation from centrosymmetry and the fact that ⟨010⟩ is the polar axis.

The R values being generally weaker for such structures, we tried to refine the enantiomorphic structure by changing all the y coordinates to $-y$. Thus we considered possible systematic errors for the measured reflections of highest θ or of weakest F_0 value; secondary extinction corrections were also made. However, none of these tests gave significant modifications in the results. It thus seems that the relatively high R value may result from incorrectly estimated absorption due to crystal shape.

Description of the Structure and Discussion

This structure is very similar to that of $P_4W_8O_{32}$, confirming that both compounds belong to the same structural family. Its framework, like that of $P_4W_8O_{32}$, consists of corner-sharing WO_6 octahedra and PO_4 tetrahedra, forming zig-zag chains parallel to the ⟨001⟩ direction and lying at the levels $y \simeq \frac{1}{4}$ and $\frac{3}{4}$ (Fig. 1). These chains are built up from two types of strings of two octahedra limited at each end by one tetrahedron, similar to those observed in $P_4W_8O_{32}$ (Fig. 2a), and strings of three octahedra limited at

TABLE IIb

ANISOTROPIC TEMPERATURE FACTORS OF THE TUNGSTEN ATOMS WITH esd's IN PARENTHESES[a]

Atom	β_{11}	β_{22}	β_{33}	β_{12}	β_{13}	β_{23}
W(1)	0.00249(15)	0.00296(33)	0.00021(1)	−0.00146(68)	0.00005(3)	−0.00009(25)
W(2)	0.00268(18)	0.00376(44)	0.00018(1)	0.00239(64)	0.00011(4)	0.00026(21)
W(3)	0.00228(16)	0.00185(37)	0.00013(1)	−0.00061(56)	0.00003(3)	0.00003(18)
W(4)	0.00309(19)	0.00220(39)	0.00025(1)	−0.00099(59)	0.00012(4)	−0.00012(21)
W(5)	0.00266(15)	0.00351(40)	0.00026(1)	−0.00003(52)	−0.00006(3)	−0.00009(16)

[a] The vibrational parameters are defined through $T = \exp\left|-\sum_i \sum_j h_i h_j \beta_{ij}\right|$.

TABLE III

Selected Interatomic Distances and Angles with Estimated Standard Deviations in Parentheses

WO$_6$ octahedra				WO$_6$ octahedra			
Distances (Å)		Angles (°)		Distances (Å)		Angles (°)	
W(1)–O(1)	1.84(2)	O(1)–W(1)–O(6A)	92.9(15)	W(5)–O(1)	1.90(3)	O(1)^a–W(5)–O(5A)^a	88.9(15)
W(1)–O(2)	1.96(2)	O(1)–W(1)–O(5B)	91.3(14)	W(5)–O(5A)^a	1.97(4)	O(1)^a–W(5)–O(14)	92.6(20)
W(1)–O(5A)	1.79(4)	O(2)–W(1)–O(5B)	91.2(14)	W(5)–O(5B)^a	1.93(3)	O(11)–W(5)–O(14)	94.3(30)
W(1)–O(5B)	1.83(3)	O(2)–W(1)–O(6A)	83.8(15)	W(5)–O(11)	1.99(4)	O(11)–W(5)–O(5A)^a	84.1(28)
W(1)–O(6A)	1.97(3)	O(5A)–W(1)–O(6B)	173.3(15)	W(5)–O(14)	1.82(5)	O(5B)^a–W(5)–O(14)^a	177.2(19)
W(1)–O(6B)	1.99(5)			W(5)–O(14)^a	1.93(5)		
⟨W(1)–O⟩	= 1.90(3)			⟨W(5)–O⟩	= 1.92(4)		
W(2)–O(3)	1.97(3)	O(3)–W(2)–O(8B)	88.9(22)				
W(2)–O(4)	1.88(3)	O(3)–W(2)–O(9B)	88.4(20)			PO$_4$ tetrahedra	
W(2)–O(8A)	1.80(4)	O(4)–W(2)–O(8B)	90.9(17)	P(1)–O(2)	1.48(3)	O(2)–P(1)–O(7A)	108.6(25)
W(2)–O(8B)	1.84(4)	O(4)–W(2)–O(9B)	91.2(15)	P(1)–O(3)	1.57(3)	O(2)–P(1)–O(7B)	109.0(27)
W(2)–O(9A)	1.90(4)	O(8A)–W(2)–O(9A)	177.3(20)	P(1)–O(7A)	1.51(5)	O(2)–P(1)–O(3)	108.1(26)
W(2)–O(9B)	1.98(4)			P(1)–O(7B)	1.53(6)	O(3)–P(1)–O(7B)	109.0(27)
⟨W(2)–O⟩	= 1.89(3)					O(7A)–P(1)–O(7B)	108.6(30)
W(3)–O(4)	1.88(3)	O(4)–W(3)–O(8A)^a	87.5(17)				
W(3)–O(8A)^a	1.95(4)	O(4)–W(3)–O(10)	92.8(14)	⟨P(1)–O⟩	= 1.52(4)		
W(3)–O(8B)^a	1.92(4)	O(13)–W(3)–O(10)	89.6(16)	P(2)–O(6A)^a	1.53(4)	O(12)–P(2)–O(6A)^a	107.6(18)
W(3)–O(10)	1.83(3)	O(13)–W(3)–O(8A)	90.0(20)	P(2)–O(6B)^a	1.55(5)	O(12)–P(2)–O(6B)^a	106.1(22)
W(3)–O(10)^a	1.93(3)	O(8B)^a–W(3)–O(10)^a	175.9(17)	P(2)–O(11)	1.53(4)	O(12)–P(2)–O(11)	107.6(35)
W(3)–O(13)	1.95(3)			P(2)–O(12)	1.51(3)	O(6A)^a–P(2)–O(6B)^a	113.9(23)
⟨W(3)–O⟩	= 1.91(3)					O(6B)^a–P(2)–O(11)	109.2(38)
W(4)–O(7A)^a	1.99(5)	O(13)–W(4)–O(7B)^a	88.6(21)	⟨P(2)–O⟩	= 1.53(4)		
W(4)–O(7B)	2.02(6)	O(13)–W(4)–O(9A)^a	96.0(19)				
W(4)–O(9A)^a	1.86(4)	O(7B)^a–W(4)–O(12)	84.5(19)				
W(4)–O(9B)^a	1.81(4)	O(12)–W(4)–O(9A)^a	90.9(17)				
W(4)–O(12)	1.99(3)	O(7A)^a–W(4)–O(9B)^a	173.7(19)				
W(4)–O(13)	1.79(3)						
⟨W(4)–O⟩	= 1.91(4)						

[a] Atom in $\bar{x}$, $1 + y$, $\bar{z}$

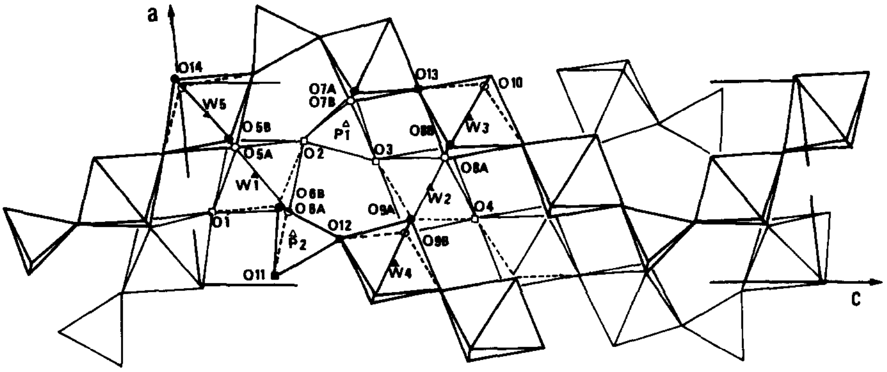

FIG. 1. Projection of the structure onto (010).

each end by one tetrahedron (Fig. 2b), corresponding to the hypothetical structure of the member $n = 3$. This structure can be described, like that of $P_4W_8O_{32}$, as ReO_3-type slabs connected through "planes" of PO_4 tetrahedra. Unlike $P_4W_8O_{32}$, two successive ReO_3-type slabs have a different width corresponding to two and three octahedra, respectively, so that the member $n = 2.5$ can be considered as an intergrowth of the two integral members $n = 2$ and $n = 3$.

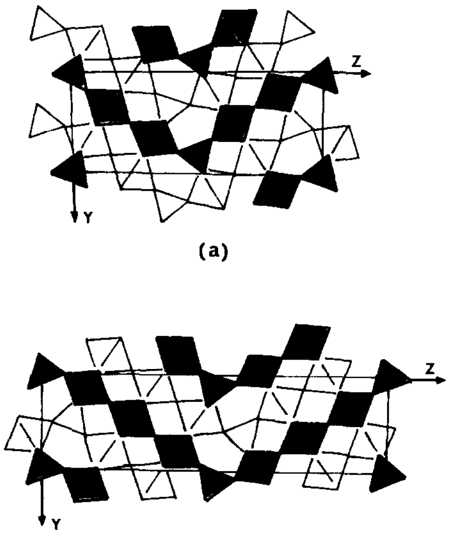

(a)

(b)

FIG. 2. The idealized structure of the terms $n = 2$ (a) and $n = 3$ (b) of the series $P_4W_{4n}O_{12n+8}$ projected along the a axis of the orthorhombic cell ($a \sim 5.3$ Å).

The two sorts of cavities of $P_4W_8O_{32}$ are also observed for $n = 2.5$. One, indeed, observes pentagonal tunnels running along the ⟨010⟩ direction, and lying in the PO_4 "planes" at the boundary between two ReO_3-type slabs.

In the same way, besides the tunnels forming "O_{18}" cages, perovskite "O_{12}" cages in which one WO_6 octahedron out of eight is replaced by one PO_4 tetrahedron are observed. Unlike $P_4W_8O_{32}$, $P_4W_{10}O_{38}$ presents true perovskite cages built up from eight octahedra owing to the presence of wider ReO_3-type slabs ($n = 3$). All these cavities are empty, as shown by the final Fourier difference series.

Among the five symmetrically independent tungsten atoms three groups of atoms can be distinguished according to their environment by the other metallic atoms: W(1) and W(4); W(2) and W(5); W(3). The $W(1)O_6$ and $W(4)O_6$ octahedra share their corners with three other octahedra and three tetrahedra in such a way that each tungsten atom is octahedrally surrounded by six metallic atoms, i.e., by 2 P(2) + 1 P(1) + 3 W(5) for W(1) and by 2 P(1) + 1 P(2) + 2 W(2) + 1 W(3) for W(4); the $W(2)O_6$ and $W(5)O_6$ octahedra are octahedrally surrounded by five octahedra and one tetrahedron, i.e., by 1 P(1) + 3 W(3) + 2 W(4) for W(2) and 1 P(2) + 3 W(1) + 2 W(5) for W(5); the $W(3)O_6$ octahedra share their corners with six other octahedra whose centers (2 W(3) + 3 W(2) + 1 W(4)) are also located at the apices of an octahedron. All the octahedra formed by the metallic atoms are almost regular in spite of the quite different nature of phosphorus and tungsten. However, their distortion increases with the number of phosphorus atoms: the W_6 octahedra are more regular than the W_5P octahedra, which are more regular than the W_3P_3. The tungsten atoms located in these metallic octahedra are more off-centered for the W_3P_3 octahedra (0.13 to 0.15 Å) than for the W_5P octahedra (0.10 to 0.11 Å) than for the W_6 octahedra (0.03 Å). This is to be compared with the results obtained for $P_4W_8O_{32}$, for which the W_3P_3 octahedra are more distorded than the W_5P octahedra, the shift of the central tungsten atom from the center of gravity being, however, about the same for both types of octahedra (0.13 Å).

In the same way, each PO_4 tetrahedron shares its corners with four WO_6 octahedra, whose center W atoms are located at the apices of an almost regular tetrahedron. The phosphorus atom is, however, farther displaced from the center of gravity of the metallic W_4 tetrahedron (0.36 to 0.39 Å); this has already been observed for $P_4W_8O_{32}$, for which the P atoms are off-centered by 0.34 Å within the W_4 tetrahedra. In return the PO_4 tetrahedra are almost regular with the phosphorus atom near the center of gravity of its tetrahedron: it is only shifted from 0.02 to 0.05 Å in agreement with the results obtained for $P_4W_8O_{32}$, in which P is off-centered of 0.07 Å. The O–O distances in the PO_4 tetrahedra ranging from 2.39 to 2.59 Å are, however, shorter than those of the WO_6 octahedra. These values are in agreement with those observed in $P_4W_8O_{38}$ (from 2.41 to 2.50 Å) and in several phosphates (*4–6*) for which O–O distances ranging from 2.43 to 2.59 Å have been observed. This confirms that the covalent character of phosphorus is preserved in $P_4W_8O_{32}$ and $P_4W_{10}O_{38}$ in spite of their metallic properties. As shown from the interatomic distances and angles given in Table III, the PO_4 tetrahedra and WO_6 octahedra are only slightly distorted. So, the O–O distances of the WO_6 octahedra range from 2.55 to 2.79 Å. However, their evolution is worthy of note: the W–O(P) distances corresponding to the W–O–P bonds are generally greater than the W–O(W) corresponding to the W–O–W bonds. W(1) and W(4) exhibit indeed a "3 + 3" coordination with three W–O(P) long distances ranging from 1.95 to 2.01 Å and three W–O(W) short distances ranging from 1.79 to 1.86 Å. In the same way the W–O(P) distances of the $W(2)O_6$ and $W(5)O_6$ octahedra, which are only linked to one PO_4 tetrahedron, are the greatest (1.97 Å), while the W–O(W) distances in the $W(3)O_6$ octahedron are more homogeneous (1.85 to 1.95 Å) owing to the fact that this octahedron is only linked to octahedra. The evolution of the O–W–O angles is correlated to the phenomenon observed for the distances: the O–W–O angles deviate more from 90° in the octahedra which are linked to PO_4 tetrahedra than in the $W(3)O_6$ octahedra which are only linked to other octahedra. This results in the tungsten atom being more off-centered in the $W(1)O_6$ and $W(4)O_6$ octahedra (0.12 to 0.13 Å) than in the $W(2)O_6$ and $W(5)O_6$ octahedra (0.07 to 0.10 Å), than in the $W(3)O_6$ octahedra (0.05 Å). This is to be compared with the results observed for $P_4W_8O_{32}$: in this oxide the $W(1)O_6$ octahedra, only linked to other octahedra, are almost regular with a displacement of W atoms from the center of gravity of 0.07 Å, while the $W(2)O_6$ octahedra which are linked to three PO_4 tetrahedra exhibit three longest W–O(P) distances (1.96 to 2.04 Å) and a greater displacement of W (0.13 Å) close to that observed in $P_4W_{10}O_{38}$.

The structural behavior of $P_4W_8O_{32}$ and $P_4W_{10}O_{38}$ must be compared with that of the γ form of the molybdenum oxide Mo_4O_{11}

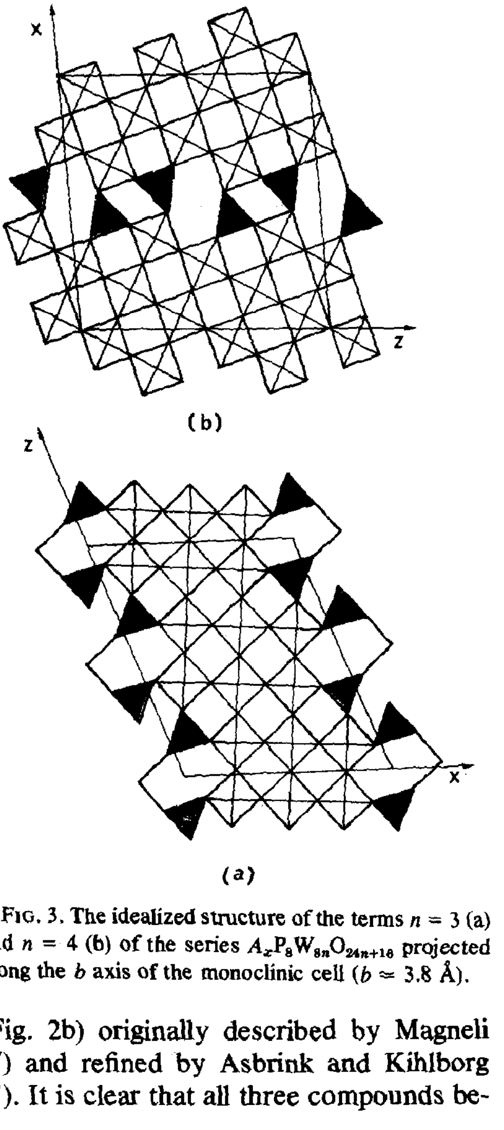

FIG. 3. The idealized structure of the terms $n = 3$ (a) and $n = 4$ (b) of the series $A_xP_8W_{8n}O_{24n+16}$ projected along the b axis of the monoclinic cell ($b \simeq 3.8$ Å).

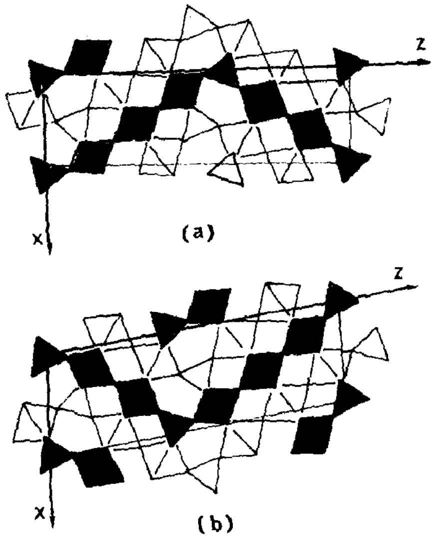

FIG. 5. The hypothetical structure of the orthorhombic form for $P_4W_{10}O_{38}$ (a) compared with the monoclinic form (b).

(Fig. 2b) originally described by Magneli (*7*) and refined by Asbrink and Kihlborg (*8*). It is clear that all three compounds belong to the same family $(M_4)_T(M_{4n})_OO_{12n+8}$ with $n = 2$ for $P_4W_8O_{32}$, $n = 3$ for γMo_4O_{11}, and $n = 2.5$ for $P_4W_{10}O_{38}$, which is, in fact, an intergrowth of $n = 2$ and $n = 3$. This lets us predict a wide field of microphases with order–disorder phenomena in the P–W–O system. An investigation is being carried out for $n \geq 3$ involving integral n values as well as nonintegral n values which would correspond to single or multiple intergrowths.

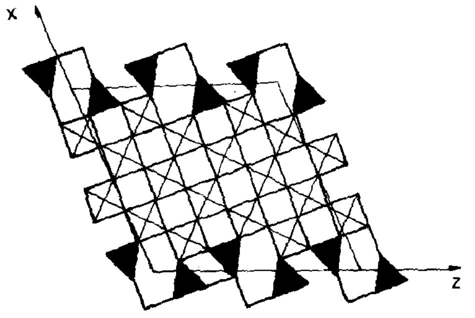

FIG. 4. The idealized $A_xP_8W_{28}O_{100}$ structure ($n = 3.5$) showing the ReO_3-type slabs.

The relation of this structural family with that of $A_xP_8W_{8n}O_{24n+16}$ (*9*) is also worthy of note. The host lattice of the latter is also built up from ReO_3-type slabs but these slabs are bounded through P_2O_7 groups forming rows of distorted hexagonal tunnels where the A ions (A = K, Rb) are located, as shown in Fig. 3a for $n = 3$ ($A_xP_8W_{24}O_{88}$) and Fig. 3b for $n = 4$ ($A_xP_8W_{32}O_{112}$). However, the study of the nonintegral member $n = 3.5$ (Fig. 4) has recently shown (*10*) that this phase is not an intergrowth of $n = 3$ and $n = 4$ which would involve a succession alternately of three and four octahedra-wide layers. It can, in fact, be considered as an original member, whose ReO_3-type layers are all identical and built up from strings of two and three octahedra, the structure of which can be deduced from the integral members $n = 3$ and $n = 4$ by a shift of two successive rows of tunnels with respect of one to the other. From these observations an orthorhombic hypothetical structure built up from identical ReO_3-type slabs can also be proposed for $P_4W_{10}O_{38}$ (Fig. 5): this form would also result from the shift of two successive rows of pentagonal tunnels with respect of one to the other, involving, for the ReO_3-type layer, a succession of strings of two and three octahedra alternately. Experiments should be considered to determine the possibility of formation of such a phase.

Conclusion

The possibility of the formation of an intergrowth in the series of oxides $P_4W_{4n}O_{12n+8}$ is demonstrated. This offers a wide field of investigation in the P–W–O system, and in a more general way in the mixed framework built up from tetrahedra and octahedra. These compounds are characterized by rather large empty cavities and the possibility of intercalation of small ions like lithium and sodium should be considered.

References

1. P. KIERKEGAARD, *Acta Chem. Scand.* **12,** 1715 (1958).
2. J. P. GIROULT, M. GOREAUD, PH. LABBE, AND B. RAVEAU, *Acta Crystallogr. Sect. B* **37,** 2139 (1981).
3. B. DOMENGES, M. GOREAUD, PH. LABBE, AND B. RAVEAU, *Acta Crystallogr.*, in press.
4. S. GHOSE, *Acta Crystallogr.* **16,** 124 (1963).
5. S. GELLER AND J. L. DURAND, *Acta Crystallogr.* **13,** 325 (1960).
6. L. O. HAGMAN AND P. KIERKEGAARD, *Acta Chem. Scand.* **22,** 1822 (1968).
7. A. MAGNÉLI, *Acta Chem. Scand.* **2,** 861 (1948).
8. S. ASBRINK AND L. KIHLBORG, *Acta Chem. Scand.* **18,** 1571 (1964).
9. J. P. GIROULT, M. GOREAUD, PH. LABBE, AND B. RAVEAU, *Acta Crystallogr. Sect. B* **36,** 2570 (1980).
10. J. P. GIROULT, M. GOREAUD, PH. LABBE, AND B. RAVEAU, *Acta Crystallogr.*, in press.